Climatic Features Related to Eastern China Summer Rainfalls in the NCAR CCM3①

Yu Rucong (宇如聪), Li Wei (李 薇), Zhang Xuehong (张学洪),
Liu Yimin (刘屹岷), Yu Yongqiang (俞永强)
Liu Hailong (刘海龙), Zhou Tianjun (周天军)

LASG, Institute of Atmospheric Physics, Chinese Academy of Sciences, Beijing 100029

(Received January 12, 2000; revised May 15, 2000)

ABSTRACT

The climatic features associated with the eastern China summer rainfalls (ECSR) are examined in the National Center for Atmospheric Research (NCAR) Community Climate Model Version 3 (CCM3) of the United States of America, and run with time-evolving sea surface temperature (SST) from September 1978 to August 1993. The CCM3 is shown to capture the salient seasonal features of ECSR. As many other climate models, however, there are some unrealistic projections of ECSR in the CCM3. The most unacceptable one is the erroneously intensified precipitation center on the east periphery of the Tibetan Plateau and its northeastward extension.

The artificial strong rainfall center is fairly assessed by comparing with the products of the station rainfall data, Xie and Arkin (1996) rainfall data and the European Centre for Medium-Range Weather Forecasts (ECMWF) reanalysis (Gibson et al., 1997). The physical processes involved in the formation of the rainfall center are discussed. The preliminary conclusion reveals that it is the overestimated sensible heating over and around the Tibetan Plateau in the CCM3 that causes the heavy rainfall. The unreal strong surface sensible heating over the southeast and northeast of Tibetan Plateau favors the forming of a powerful subtropical anticyclone over the eastern China. The fake enclosed subtropical anticyclone center makes the moist southwest wind fasten on the east periphery of the Tibetan Plateau and extend to its northeast. In the southeast coast of China, locating on the southeast side of the subtropical anticyclone, the southwest monsoon is decreased and even replaced by northeast wind in some cases. In the CCM3, therefore, the precipitation is exaggerated on the east periphery of the Tibetan Plateau and its northeast extension and is underestimated in the southeast coast of China.

Key words: Eastern China summer rainfall, Model validation, Subtropical anticyclone, Diabatic heating

1. Introduction

The broadly defined Asian monsoon actually consists of the Indian monsoon and the East Asian monsoon. The Indian summer monsoon, as well as its connection with some other climatic variabilities, such as the ENSO event, has been studied extensively (Rasmusson and Carpenter, 1983; Shukla and Paolino, 1983; Shukla and Mooley, 1987; Ju and Slingo, 1995). To the East Asian monsoon, with its main part over the eastern China, its relationship with

①This study was sponsored by Chinese Academy of Sciences under grant "Hundred Talents" for "Validation of Coupled Climate models" and the National Natural Science Foundation of China (Grant No.49823002), and IAP innovation fund (No. 8-1204).

ENSO and other large scale climatic systems is more complex than that for the Indian monsoon due to the effect of complex geography of South Asia, the steep orography of the Tibetan Plateau, and the sharp heating gradients. This is the reason why the eastern Asian monsoon is often ignored in many Asian monsoon studies.

To the present, quantitative study of the monsoon system resorts primarily to the numerical simulation by atmospheric general circulation models (AGCMs). Skills of different AGCMs in simulating the monsoon are compared in the WCRP Atmospheric Model Intercomparison Project (AMIP) (Gates, 1992; Gates et al., 1992) with an overall unsatisfied evaluation. Almost all of the AGCMs, including CCM3, have unacceptable features in simulating the complex East Asian monsoon.

Meehl and Arblaster (1998) indicated that the NCAR Climate System Model(CSM) and CCM3 are able to represent most major features of the Asian–Australian monsoon system. However, the research still focuses on the Indian monsoon and Australian monsoon without the East Asian monsoon being mentioned. From Fig. 1 in Meehl and Arblaster (1998), it is found that the CCM3 really has an unsatisfied simulation to the summer rainfall amounts over the eastern China. To improve the ability of AGCMs in simulating the East Asian monsoon system, it is necessary to evaluate the current model ability by detecting the unrealistic simulation and probing the causes. In the present paper, the major climatic features related to ECSR, an important projection of East Asian summer monsoon, in the CCM3 are shown and compared with observations as a compensation for Meehl and Arblaster (1998).

This paper is organized as follows. Section 2 describes the model (CCM3) and data sets. In Section 3, we examine the mean seasonal climatic features of ECSR. Section 4 discusses the relationships between the simulated rainfall and circulation in order to reveal the physical linkages in the unsatisfied simulations. Section 5 is a brief summary.

2. Model and data description

CCM3, the last version of the National Center for Atmospheric Research (NCAR) Community Climate Model (CCM), is a stable, efficient, documented and state of the art global spectral AGCM, with a horizontal T42 spectral resolution (approximately $2.8° \times 2.8°$ transform grid) and 18 levels in the vertical, designed for climate research (Kiehl et al., 1996; Kiehl et al., 1998). From CCM2, the previous version of CCM, to CCM3, the major improvements include the parameterization of cloud properties, clear sky longwave radiation, deep convection, boundary layer processes, and land surface processes. These modifications have led to dramatic improvements in the simulated climate of the CCM. The CCM3 is shown to represent most major features of the Asian–Australian monsoon system in terms of mean climatology, interannual variability, and connections with the tropical Pacific (Meehl and Arblaster, 1998).

The data used to assess the CCM3 in the present study include the widely used Xie and Arkin (1996) rainfall data, the monthly station rainfalls from 115 stations over the eastern China from January 1951 to December 1998, which is compiled by China Meteorological Administration, and the European Centre for Medium–Range Weather Forecasts (ECMWF) reanalysis products (Gibson et al., 1997). The National Center for Environmental Prediction (NCEP)/ NCAR reanalysis (Kalnay et al., 1996) is also mentioned. But, for the shown features, the results based on the two reanalysis products are very similar to each other, so the results from the NCEP/ NCAR reanalysis are not given.

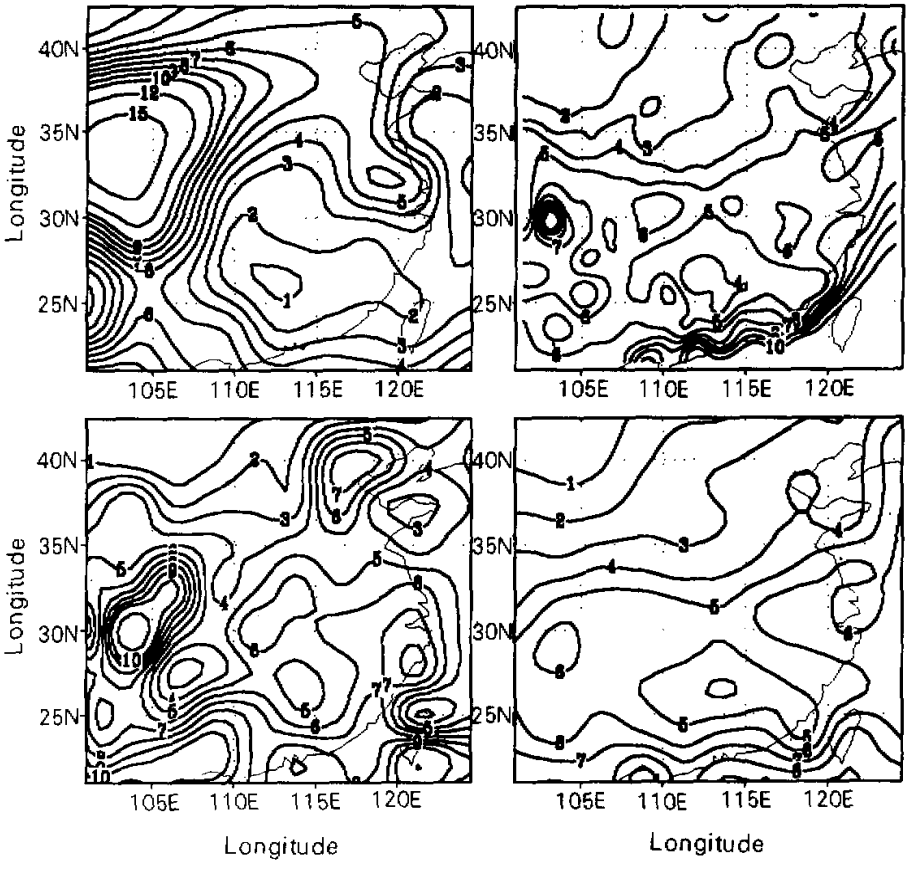

Fig. 1. Time-mean precipitation for June / July / August (JJA) 1983–1992 over eastern China based on the CCM3 integration (a), monthly station rainfall data (b), ECMWF reanalysis (c) and Xie and Arkin's gridded data (d).

3. Mean and seasonal climatic features

The 10-year (1983–1992) mean climatology of precipitation from June to August (JJA) average over the eastern China is shown in Fig. 1 for the CCM3 (Fig. 1a) compared with the analyses, which are obtained from monthly station rainfall data (Fig. 1b), ECMWF reanalysis (Fig. 1c) and Xie and Arkin (1996) gridded precipitation data (Fig. 1d) respectively. It is expected that major precipitation pattern shows remarkably good agreement between Fig. 1b and Fig. 1d except for the more smoothed distribution in Fig. 1d while more rainfall centers in Fig. 1b. It can be concluded that Xie and Arkin's (1996) rainfall data are reliable with regard to representing the mean climate of rainfall in the eastern China. Some small precipitation centers cannot be identified in Xie and Arkin's data partly due to its coarse resolution. Some small strong precipitation centers, such as a topography-related one locating on the east periphery of the Tibetan Plateau (Ya-An, 103°E, 30°N) being of extreme annual

rainfall amount (in excess of 1600 mm) over very small area (about 100 km^2), have important climate significance.

One obvious feature exhibited in Fig. 1b or Fig. 1d is that the summer rainfall belt extends along the Yangtze River (around 30°N), and the precipitation over South China is relatively weak with the exception of the coastal line. The pattern in Fig. 1a has similar feature to that in Fig. 1b with heavy rainfall in the northern part and weak precipitation in the south, although the rainfall amount in Fig. 1a has a significant deviation from the observation. The mean climate to ECMWF reanalysis, in which the daily rainfall is the sum of 4 times accumulated precipitation from 6 hours running of the ECMWF T106 AGCM and interpolated to the grid of 2.5° longitude by 2.5° latitude, is also given for comparison. The intensity of precipitation center on the east periphery of the Tibetan Plateau is also exaggerated extremely although it is better than the case to CCM3. There is similar exaggerated rainfall center in the NCAR / NCEP reanalysis too (not shown).

As we know, there is a close relationship between the variability of East Asian summer rainfall and the summer monsoon circulation. On the upper level (100 hPa), the CCM3 (Fig. 2b) qualitatively reproduces the general structure of the subtropical anticyclone based on ECMWF reanalysis (Fig. 2a), with the principal part on the Eurasia, the axis of subtropical anticyclone along 30°N, westerly jet along 40°N and easterly wind to the south of 25°N.

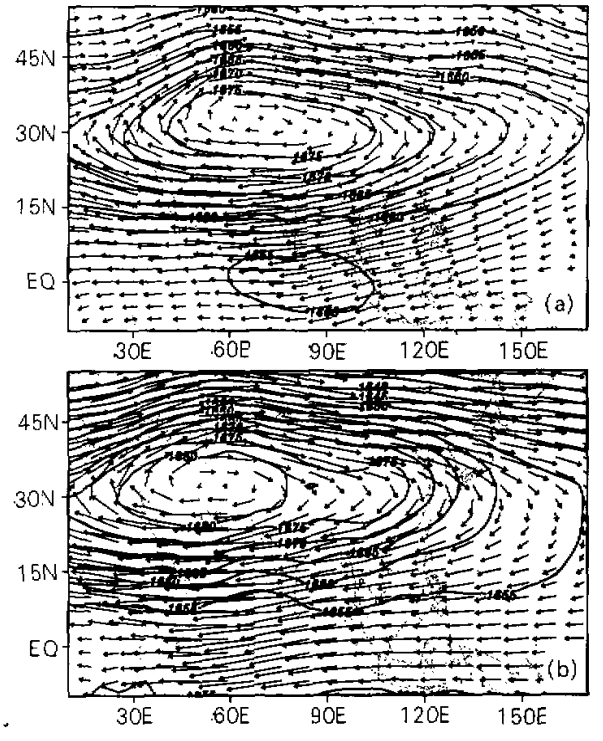

Fig. 2. JJA mean horizontal wind fields at 100 hPa from ECMWF reanalysis (a) and the CCM3 (b). Also shown are the contours of geopotential height (unit: ten geopotential meters).

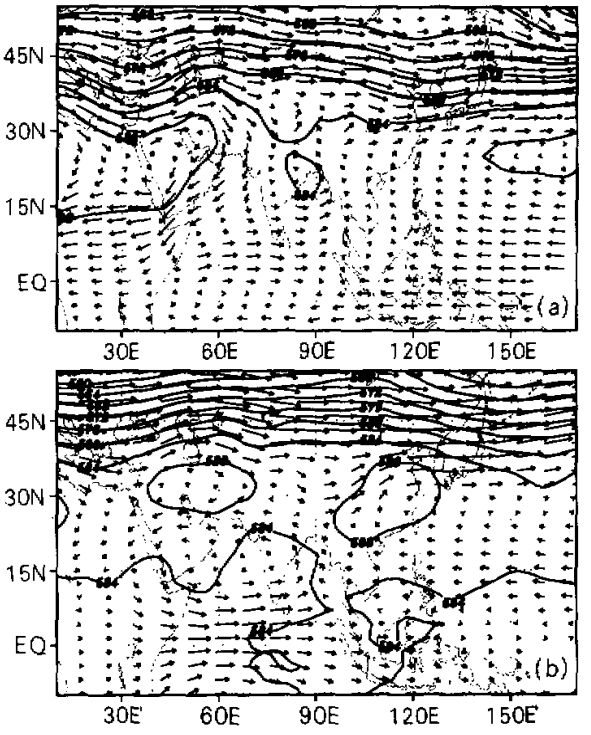

Fig. 3. As in Fig. 2, but for 500 hPa.

On the middle or lower level (500 hPa), the axis of subtropical high in the CCM3 (Fig. 3b) is around 25°N as that in ECMWF reanalysis (Fig. 3a). A noticeable difference is found that the center of subtropical high lies in Eurasia for the CCM3 rather than over the Pacific for the observed (Fig. 3a vs 3b). One erroneously powerful high center settles in the eastern China, which makes the moist southwest wind fasten on the east periphery of the Tibetan Plateau and strongly extend to its northeast. To the southeast coast of China, below 500 hPa, the southwest wind is decreased and even replaced by northeast wind. In the CCM3, therefore, the precipitation over the east periphery of the Tibetan Plateau and its extension to the northeast is exaggerated, and the precipitation in the southeast coast of China is underestimated.

A typical characteristic of ECSR is the northward jump of the rainfall belt and related circulation, such as subtropical anticyclone, around June and July. Two contour lines, 5800 and 5880 geopotential meters (gpm), on 500 hPa averaged for 10 years (1983–1992) from May to August based on ECMWF reanalysis are shown in Fig. 4a. The contour of 3 mm / day precipitation rates, analyzed from Xie and Arkin's rainfall data for the same period, is shown in Fig. 4b. The same 5800 gpm and 5880 gpm contour lines and both 5 mm / day and 10 mm / day precipitation rates in the CCM3 are shown in Fig. 5a and Fig. 5b respectively for comparison. It can be seen that, for the 10-year mean climate, the CCM3 captures the two obviously northward movements of the rainfall belt and subtropical high

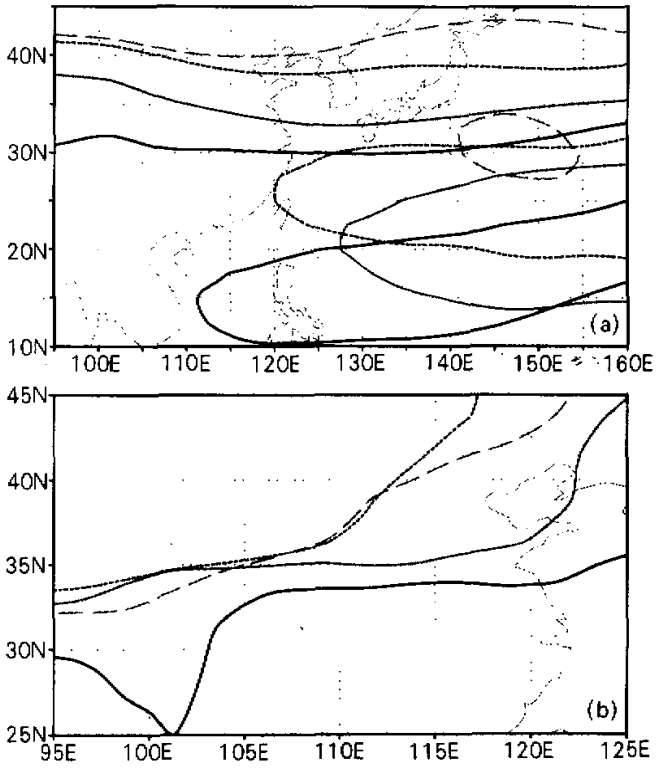

Fig. 4. 5800 and 5880 gpm contour lines on 500 hPa based on ECMWF reanalysis(a) and the contour of 3 mm / day precipitation rates from Xie and Arkin rainfall data (b), averaged for May (heavy solid lines), June (thin solid lines), July (dotted lines) and August(dashed lines) 1983–1992.

belt in June and July as those exhibited in the observed, although with a significant deviation. The representation to the two sudden displacements, which have a great impact on ECSR, in the CCM3 confirms that the model does a reasonable job in producing the basic evolution of the main systems in East Asian climate.

4. Discussions

4.1 *The heavy rainfalls on the east periphery of Tibetan Plateau*

As mentioned in Section 3, it seems that the major departure of the modeling ECSR is that the CCM3 exaggerated the intensity and area of the precipitation center on the east periphery of the Tibetan Plateau. To understand the physical processes for the CCM3 to simulate huge rainfall amounts over the eastern China, it should be helpful to examine the cause of formation of observed strong climatological rainfall center in the small area on the east periphery of the Tibetan Plateau.

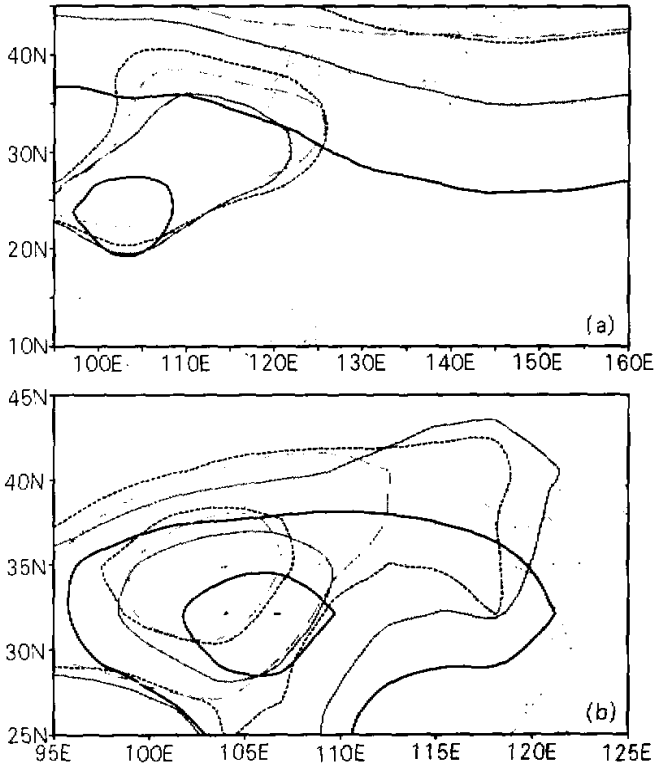

Fig. 5. As in Fig. 4 but (a) for the CCM3 and (b) for both the 5 mm / day and 10 mm / day precipitation rates in the CCM3.

The observed small rainfall center is over the Ya–An (YA) district, around (103°E, 30°N) on the west edge of Sichuan Basin of China or the east periphery of the Tibetan Plateau, marked by heavy black dots in Fig. 6a and Fig. 6b. Fig. 6 shows the topography over the eastern China with the real terrain analyzed from 0.5° × 0.5° resolution data in Fig. 6a and the CCM3 terrain in Fig. 6b. YA (103°E, 30°N) is located on the angled point of the trumpet orography with Sichuan Basin, symbolized by 500 m contour, to its east. The heavy rainfall over YA is a typical terrain influencing precipitation. In Chinese, the so-called "Ya–An Tian–Lou" (YATL) means that the sky over YA district has a leaking hole in keeping raining.

YATL has been studied for many years by Chinese meteorologists as a special precipitation phenomenon. It is influenced by the topography in not only dynamic but also thermodynamic aspects. A possible mechanism of the heavy rainfall on the east periphery of the Tibetan Plateau has been suggested by case studies (e.g. Yu and Zeng, 1992; Yu et al., 1994; Zeng et al. 1994). It is noted that the sensible heat flux at the east steep slope of the Tibetan Plateau heats the air above the slope, which makes it warmer than ambient air at the same altitude. The warmed air in the YA trumpet terrain region moves upward while the air

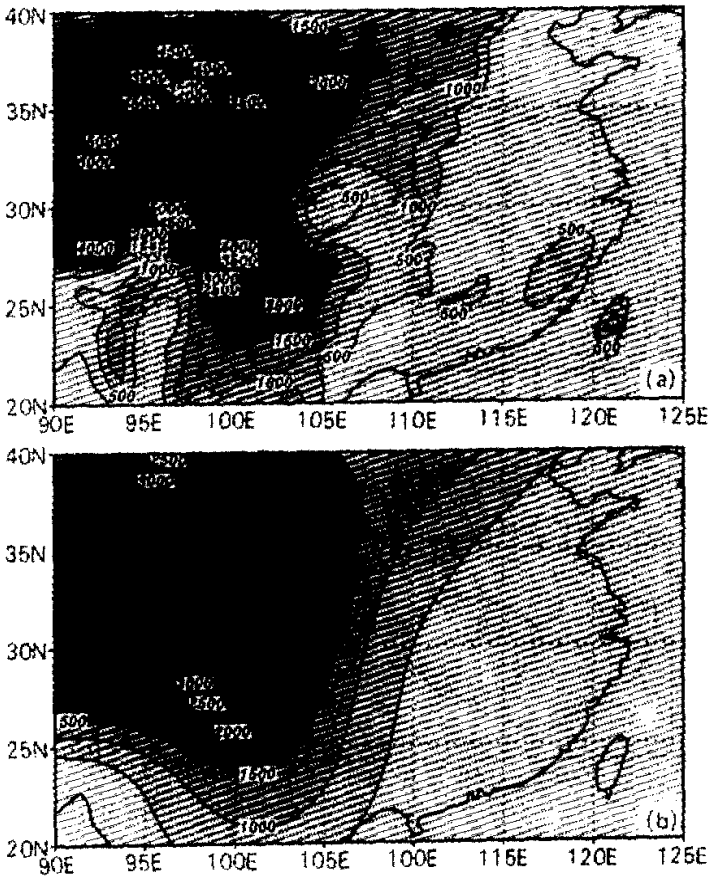

Fig. 6. The topography over the eastern China with real terrain analyzed by 0.5° × 0.5° resolution data (a) and CCM3 terrain (b). A black dot marks Ya–An (103°E, 30°N) for the both.

over the Sichuan Basin flows westward and climbs along the slope, forming a low–level vertical circulation on the east periphery of the Tibetan Plateau. In addition, the Tibetan Plateau is dominated by upward air motion in summer because of the powerful sensible heating, which has advantage of pumping the air from the east slope and intensifying the upward motion. The retraced moist monsoon air gets concentrated during the vertical motion in the YA area. The more condensation, the more latent heating, and the stronger upward motion is. Partly because of the coarse horizontal resolution, the CCM3 (Fig. 6b) cannot capture the terrain characteristics in the Sichuan Basin and the east steep trumpet slope of the Tibetan Plateau, which limits the rainfall amount at the small area in the west of Sichuan Basin (Fig. 6a).

Fig. 7 shows the 10 years (1983–1992) mean zonal–vertical circulation averaged for JJA over the rainfall center on the east periphery of the Tibetan Plateau. The ECMWF reanalysis exhibits strong upward motion near the YA district in Fig. 7a. This is also the case for the CCM3 (Fig. 7b), only that the intensity of the vertical motion is much stronger than that from the reanalysis. Additionally, there are some more similar features between the simulated

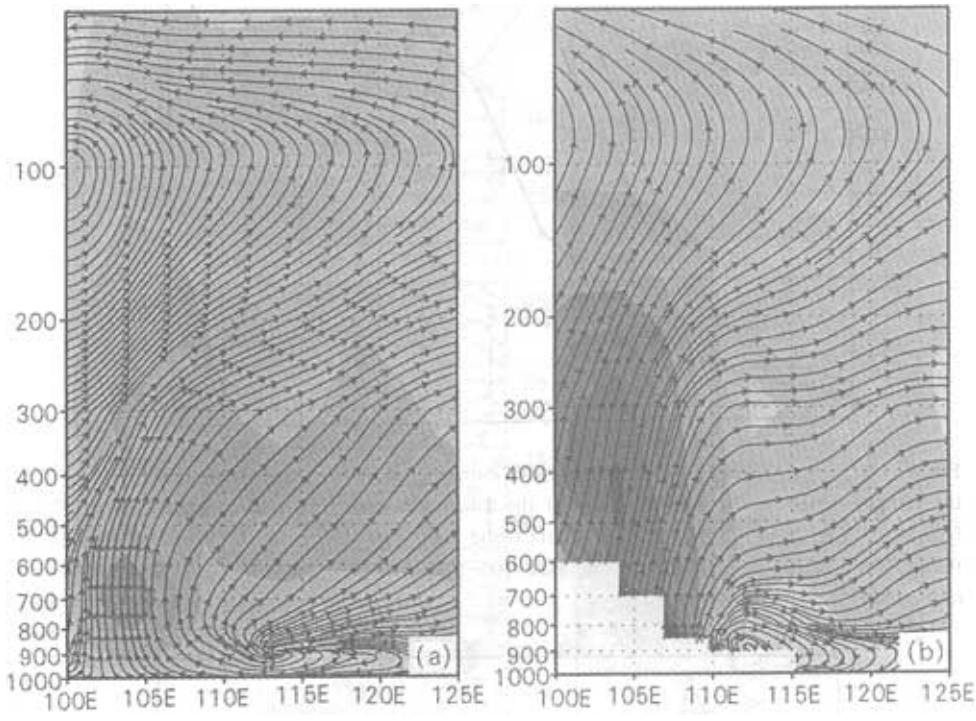

Fig. 7. 10-year (1983–1992) mean zonal-vertical circulation for JJA average over the eastern China from the ECMWF reanalysis at 30°N (a) and the CCM3 at 32°N (b). The vertical motion is shaded to highlight the strong upward motion.

rainfall center in Fig. 1a and the observed YATL in Fig. 1b. The 10 years (1983–1992) mean climatologies of monthly precipitation rates in mm / day for the rainfall center on the east periphery of the Tibetan Plateau are shown in Fig. 8. For the station data (solid line), the average is over 102.5–103.5°E, 29.5–30.5°N. For the ECMWF reanalysis (dashed line), it is 102.5–105°E, 28.5–31.5°N. The CCM3 (dotted line) is over 100–105°E, 30–37°N. The three lines in Fig. 8 have approximately the same precipitation rate maxima, and the rainy season are mainly in summer. But the rainy season in both the ECMWF reanalysis and the CCM3 is from May to September, longer than that in the station observation (in July and August).

Fig. 9 shows the abnormal interannual variability of JJA rainfalls, averaged over the east periphery of the Tibetan Plateau, during the 10 years (1983–1992) in the station observation (solid line), the ECMWF reanalysis (dashed line) and the CCM3 (dotted line). There is a suggestion that some consensus exists on the three rainfall time series. Corresponding to three positive peaks in the station observation, the CCM3 and ECMWF reanalysis also have positive anomalies.

Based on above discussion, the strong rainfall center on the east periphery of the Tibetan Plateau in the CCM3 and ECMWF reanalysis has similar features to the YATL except for the larger spacial distribution and strong intensity. In the following sub-section, attention is paid to explain the cause of simulated huge rainfall center. The huge intensified precipitation is connected with the circulation driven by sensible heating and convective latent heating around the Tibetan Plateau.

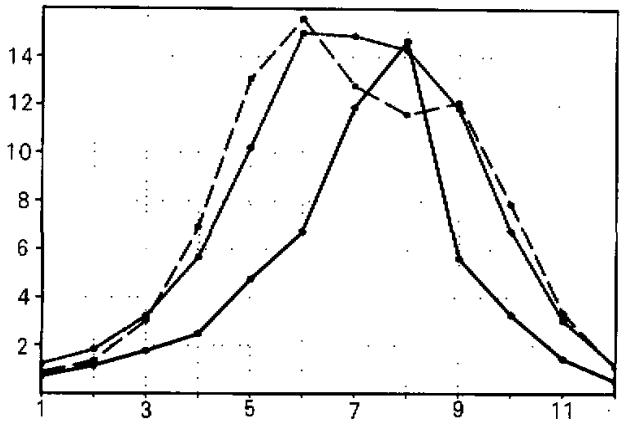

Fig. 8. The 10-year (1983–1992) mean climate of monthly precipitation rates (unit: mm / day) for the rainfall center on the east periphery of the Tibetan Plateau. The center is averaged over (102.5–103.5°E, 29.5–30.5°N) for station data (solid line), over (102.5–105°E, 28.5–31.5°N) for the ECMWF reanalysis (dashed line) and over (100–105°E, 30–37°N) for the CCM3 integration (dotted line).

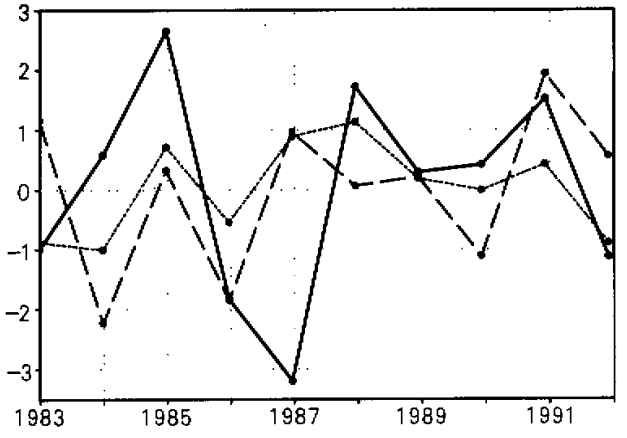

Fig. 9. The anomaly of interannual variations of JJA rainfalls from 1983 to 1992, averaged over areas same as that in Fig. 8, for the station observation (solid line), the ECMWF reanalysis (dashed line) and the CCM3 (dotted line).

4.2 *The diabatic heating in driving the circulation and precipitation*

There is a very tight coupling between the eastern Asian monsoon circulation and the diabatic processes. The monsoon circulation is driven by the diabatic processes, particularly by the sensible heating and deep convection heating, and at the same time the diabatic processes are influenced by the monsoon circulation.

Fig. 10 shows the monthly sensible heat flux (shaded), 10 mm / day contour line of precipitation rate (dotted line), 5880 gpm contour line on 500 hPa (solid line), 3160 gpm contour

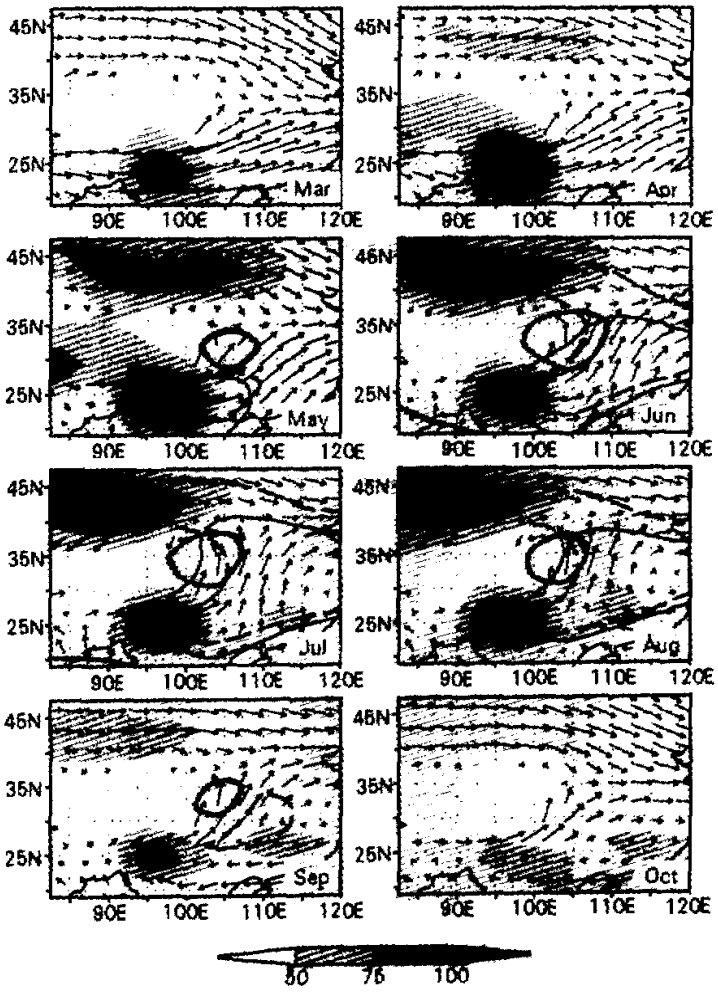

Fig. 10. Monthly mean sensible heat flux (shaded), 10 mm / day contour line of precipitation rate (dotted line), 5880 gpm contour line on 500 hPa (solid line), 3160 gpm contour line on 700 hPa (dashed line), and horizontal winds at 700 hPa (vector), averaged for March to October 1983–1992 from the CCM3.

line on 700 hPa (dashed line) and horizontal winds at 700 hPa (vector), averaged from March to October 1983–1992. It is clear that, in summer, two strong surface sensible heating centers are on the southeast and northeast periphery of the Tibetan Plateau. The mid–lower level high center is on the east of the sensible heating centers with two high ridges toward or over them. The precipitation center is located at the center of the triangle formed by two heating centers and one high center. Fig. 11 shows the 10 years mean monthly sensible heat fluxes averaged over the region of 93–100°E, 21–27°N, precipitation rates averaged over

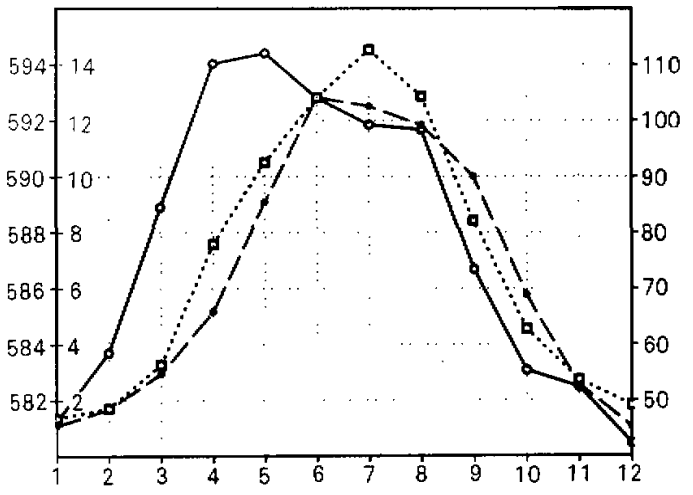

Fig. 11. The 10-year mean monthly sensible heat fluxes averaged over the region of (93–100°E, 21–27°N, solid line), precipitation rates averaged over (100–105°E, 30–37°N, dashed line), and the 10-year mean maximum of 500 hPa geopotential height over (90–125°E, 20–40°N, dotted line).

100–105°E, 30–37°N, and the 10-year mean maximum of geopotential height at 500 hPa over 90–125°E, 20–40°N. Referring to Fig. 10 and Fig. 11, the variability of the sensible heating center, such as that over the southeast periphery of the Tibetan Plateau, leads the subtropical high and precipitation center by one or two months. The high forms in the northeast or the leeward of the heating center in April and May at beginning. Then the high develops intensively and extends northeastward. Following another heating center appears in the northeast periphery of the Tibetan plateau, the high extension turns to northwest and forms a ridge over the heating center from June. Therefore, the southwest monsoon and the cyclone circulation are intensified on the east periphery of the Tibetan Plateau in the mid-lower level, which benefits the forming of heavy rainfall. Meanwhile, the southwest monsoon is decreased and even replaced by northeast wind in the south coast of China, which is located on the southeast side of the subtropical anticyclone. The precipitation also weakens there.

The unrealistic strong precipitation on the east periphery of the Tibetan Plateau in the CCM3 simulation is qualitatively analyzed by the relationship between sensible heating and circulation. In the following part of this section, the physics about how the surface sensible heating has an effect on the subtropical anticyclone or circulation is studied based on the complete form of vertical vorticity tendency equation (Wu and Liu, 1997, Wu et al., 1999).

Wu et al. (1999) and Liu et al. (1999a, b) studied the nonuniform diabatic heating influence on the formation and variability of subtropical anticyclone based on the complete form of vertical vorticity tendency equation. The main conclusion is that the vertical nonuniform diabatic heating has great impacts on the formation of the enclosed subtropical anticyclone centers. The relative stabilization of the western Pacific subtropical anticyclone and high level South Asia high was discussed. The vertical vorticity tendency equation influenced by nonuniform diabatic heating can be written as

$$\frac{\partial \zeta}{\partial t} + \vec{V} \cdot \nabla\zeta + \beta v = \frac{f + \zeta}{\theta_z} \frac{\partial}{\partial z}(Q_{sh} + Q_{lh}) . \quad (1)$$

where ζ is the vertical component of relative vorticity, θ is the potential temperature, $\theta_z = \partial\theta / \partial z$ determines static stability, Q_{sh} and Q_{lh} are the sensible and latent heating rates, respectively.

The 10 years mean JJA averaged vertical profile of sensible heating rate in the southeast of Tibetan Plateau (93–100°E, 21–27°N) is shown in Fig. 12a, and the latent heating rate in the east of the Tibetan Plateau (100–105°E, 30–37°N) is shown in Fig. 12b. Based on Eq.(1), the sensible heating, which sharply decreases from surface to 500 hPa, is beneficial to forming an anticyclone high in the middle and lower levels above the heating area as shown in Fig. 10. To the long time scale, the local variation of ζ may be ignored, then

$$\vec{V} \cdot \nabla\zeta + \beta v < 0 .$$

In this southwest monsoon region, $\beta v > 0$. So it must be $\vec{V} \cdot \nabla\zeta < 0$. This situation favors the forming of an anticyclone high in the leeward area as shown in Fig. 10 and a cyclone low in the windward area (not shown in Fig. 10). For the sensible heating in the northeast of Tibetan Plateau, v is close to zero, $\vec{V} \cdot \nabla\zeta$ is still less than 0, which results in a high ridge toward and over the heating area. In addition, the latent heating shown in Fig. 12b is of the advantage of intensifying the anticyclone high in its east from 700 hPa to 250 hPa.

According to the discussion, the unrealistic strong diabatic heating around the eastern Tibetan Plateau determines the unreal circulation and precipitation on the east periphery of the Tibetan Plateau. It can be further confirmed by comparing the results in the reanalysis products. Fig. 13 shows the connection between the sensible heating and precipitation in the

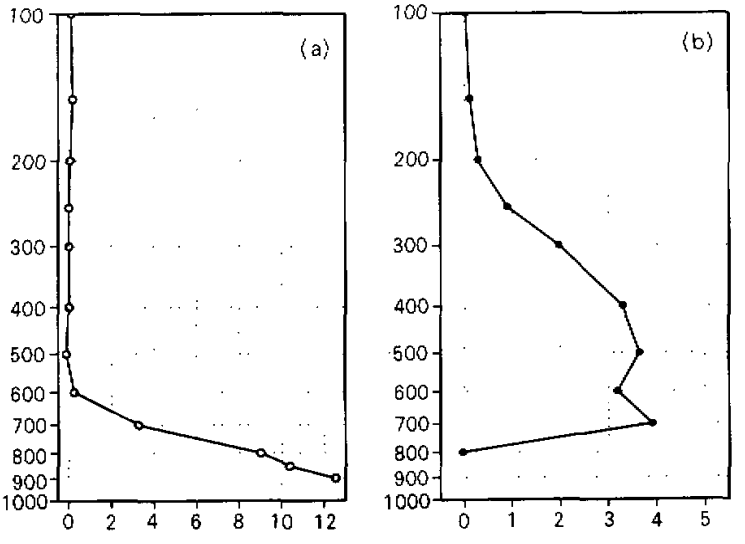

Fig. 12. Vertical profiles of sensible heating rate in the southeast of Tibetan Plateau (93–100°E, 21–27°N) (a) and the latent heating rate in the east of Tibetan Plateau (100–105°E, 30–37°N) (b) averaged for JJA in 10 years from the CCM3.

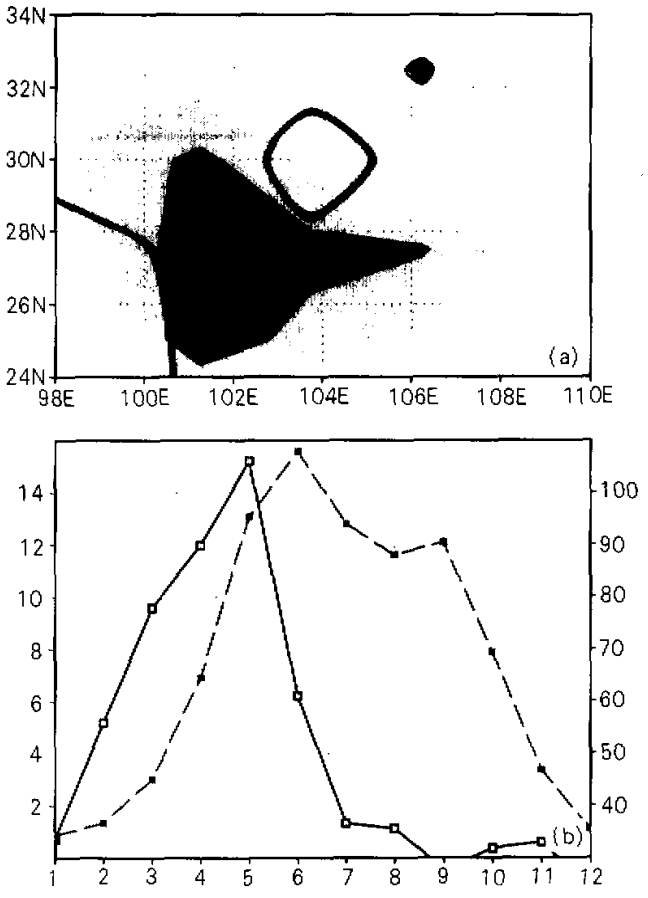

Fig. 13. The 10-year mean sensible heating and precipitation from the ECMWF reanalysis. (a) March–April–May mean sensible heating (shaded) and JJA mean 10 mm/day contour line of precipitation rate (heavy lines), (b) monthly sensible heat fluxes averaged over the region of (100.5–102.5°E, 26.5–29.5°N, solid line) and precipitation rates averaged over the region of (102.5–105°E, 28.5–31.5°N, dashed line).

ECMWF reanalysis. The pattern of heating–rainfall distribution (Fig. 13a) is the same as that in the CCM3 (Fig. 10). The sensible heating maximum leads the maximum of precipitation rate by one month (Fig. 13b).

5. Conclusions

In this study, based on the station monthly rainfall data, Xie and Arkin monthly rainfall data and ECMWF reanalysis, the climatic features of ECSR in the CCM3 are evaluated. The CCM3 is verified to be able to capture the major characteristics of the rainfall distribution and the seasonal climatic features. From Fig. 2, Fig. 3 and Fig. 7, the CCM3 also reproduces the circulation of the eastern Asian summer monsoon quite well. As many other climate mod-

els, there are some unsatisfied projections of ECSR in the CCM3. The most unacceptable features are the extremely overestimated rainfall center on the east periphery of the Tibetan Plateau, which is related to the overestimated surface sensible heat flux around the Tibetan Plateau and unrealistic subtropical high over the eastern China.

It seems that the huge precipitation center on the east periphery of the Tibetan Plateau could be the exaggerated YATL, which is influenced by special topography in both dynamic and thermodynamic aspects. Partly because of the coarse horizontal resolution, the CCM3 cannot capture the terrain characteristic in the Sichuan Basin of China and the east steep slope of the Tibetan Plateau, which has an effect on the limitation of the heavy rainfall on the small area in the west of Sichuan Basin. The overestimated surface sensible heating around Tibetan Plateau has advantage to form the anticyclone high over the eastern China following the vertical vorticity equation. The high intensifies the moist southwest monsoon and the monsoon–related precipitation on the northwest part of the eastern China, and weakens the southwest monsoon as well as the precipitation on the southeast part of the eastern China. In addition, there is a positive feedback between the strong rainfall latent heating and the anticyclone high to its east.

The aforementioned unrealistic projections of ECSR exist not only in the CCM3 but also in the other AGCMs, including the NCAR / NCEP and ECMWF reanalysis of ECSR which reveals a great influence of the complex sub–grid topography on the local climate. It is hoped that the present study will provide some motivations to pay much attention to the topography influence and related land surface processes in the future model validation.

REFERENCES

Gates, W. L., 1992: AMIP: The Atmospheric Model Intercomparison Project. *Bull. Amer. Meteor. Soc.*, **73**, 1962–1970.

Gates, W. L., J. F. B. Mitchell, G. J. Boer, U. Cubasch, and V. P. Meleshko, 1992: Climate modelling, climate prediction and model validation. In: *Climate Change, The Supplementary Report to the IPCC Scientific Assessment*, J. T. Houghton, B.A.Callander and S. K. Varney (eds), Cambridge University Press, Cambridge, UK, 97–134.

Gibson, J. K., P. Kallberg, S. Uppala, A. Hernandez, A. Nomura and E. Serrano, 1997: ERA description. ECMWF Reanalysis Project Report Series 1, European Centre for Medium Range Weather Forecasts, Reading, UK, 66 pp.

Ju, J. and J. Slingo, 1995: The Asian monsoon and ENSO. *Quart. J. Roy. Meteor. Soc.*, **121**, 1133–1168.

Kalnay, E., and Coauthors, 1996: The NCEP/NCAR 40-year reanalysis project. *Bull. Amer. Meteor. Soc.*, 77, 437–471.

Kiehl, J. T., J. J. Hack, G. B. Bonan, B. A. Boville, D. L. Williamson, and P. J. Rasch, 1998: The National Center for Atmospheric Research Community Climate Model: CCM3. *J. Climate*, **11**, 1131–1149.

Kiehl, J. T., J. J. Hack, G. B. Bonan, B. A. Boville, B. P. Briegleb, D. L. Williamson, and P. J. Rasch, 1996: Description of the NCAR Community Climate Model (CCM3). NCAR Tech. Note, NCAR / TN–420+SRT, 152 pp. [Available from National Center for Atmospheric Research, Boulder, CO 80307.]

Liu, Y. M., H. Liu, P. Liu, G. X. Wu, 1999a: The effect of spatially nonuniform heating on the formation and variation of subtropical high. II : Land surface sensible heating and East Pacific subtropical high. *Acta Meteorologica Sinica*, **57**, 385–396 (in Chinese).

Liu, Y. M., G. X. Wu, H. Liu, P. Liu, 1999b: The effect of spatially nonuniform heating on the formation and variation of subtropical high, III : Condensation heating and South Asia high and western Pacific subtropical high. *Acta Meteorologica Sinica*, **57**, 525–538 (in Chinese).

Meehl, G. A., and J. M. Arblaster, 1998: The Asian–Australian monsoon and El Niño–Southern Oscillation in the NCAR Climate System Model. *J. Climate*, **11**, 1356–1385.

Rasmusson, M., and T. H. Carpenter, 1983: The relationship between eastern equatorial Pacific sea surface temperature and rainfall over India and Sri Lanka. *Mon. Wea. Rev.*, **111**, 517–528.

Shukla, J., and D. A. Mooley, 1987: Empirical prediction of the summer rainfall over India. *Mon. Wea. Rev.*, **115**, 695–703.

Shukla, J., and D. A. Paolino, 1983: The Southern Oscillation and long range forecasting of the summer monsoon rainfall over India. *Mon. Wea. Rev.*, **111**, 1830–1837.

Wu, G. X., and H. Z. Liu, 1997: Vertical vorticity development owing to down-sliding at slantwise isentropic surface. *Dyn. Atmos. Oceans*, **27**, 715–743.

Wu, G. X., Y. M. Liu, and P. Liu, 1999: The effect of spatially nonuniform heating on the formation and variation of subtropical high. I : Scale analysis. *Acta Meteorologica Sinica*, **57**, 257–263 (in Chinese).

Xie, P., and P. A. Arkin, 1996: Analyses of global monthly precipitation using gauge observations, satellite estimates and numerical model predictions. *J. Climate*, **9**, 840–858.

Yu, R. C., and Q. C. Zeng, 1992: The design of a limited area model with steep mountains and its application to the heavy rain simulations in the east periphery of Tibetan Plateau. 22nd International Conference on Alpine Meteorology, Toulouse, France, 7–11 September 1992, 316–320.

Yu, R. C., Q. C. Zeng, G. K. Pong, and F. X. Chai, 1994: Heavy rainfalls over Yaan. Part 2: Numerical trial-forecasting. *Scientia Atmospherica Sinica*, **18**, 535–551 (in Chinese).

Zeng, Q. C., R. C. Yu, G. K. Pong, and F. X. Chai, 1994: Heavy rainfalls over Yaan. Part 3: Structure and mechanism. *Scientia Atmospherica Sinica*, **18**, 649–659 (in Chinese).